

Figure 9. The flatness of u -fluctuation at (a) $X/h = 1.5, 4.0,$ and 6.5 (near and upstream of reattachment location) and (b) at $X/h = 9.0$ (downstream of reattachment) for both excited and unexcited cases.

Comparing figures 8 and 9 with figures 2 and 3, it may be seen that the Y/h locations having non-Gaussian distribution (higher value of skewness and flatness) correspond to the upper part of the shear layer, i.e. the region from maximum turbulence intensity to the edge of the shear layer. It should be mentioned that earlier (Panigrahi 2001), significant ejection motion was observed in the outer shear layer region. In the upper part of the shear layer, entrainment takes place in the form of large-scale engulfment of non-vortical fluid near the interface. These intermittent large-scale entrainment motions may be the primary cause for higher values of skewness and flatness at these locations. To determine if there is a correlation between the ejection motion and higher order moments, the Y/h locations corresponding to the maximum values of skewness and flatness and maximum average hole size of the ejection motion for both excited and unexcited cases are presented in table 1. It may be seen from table 1 that the Y/h locations are almost

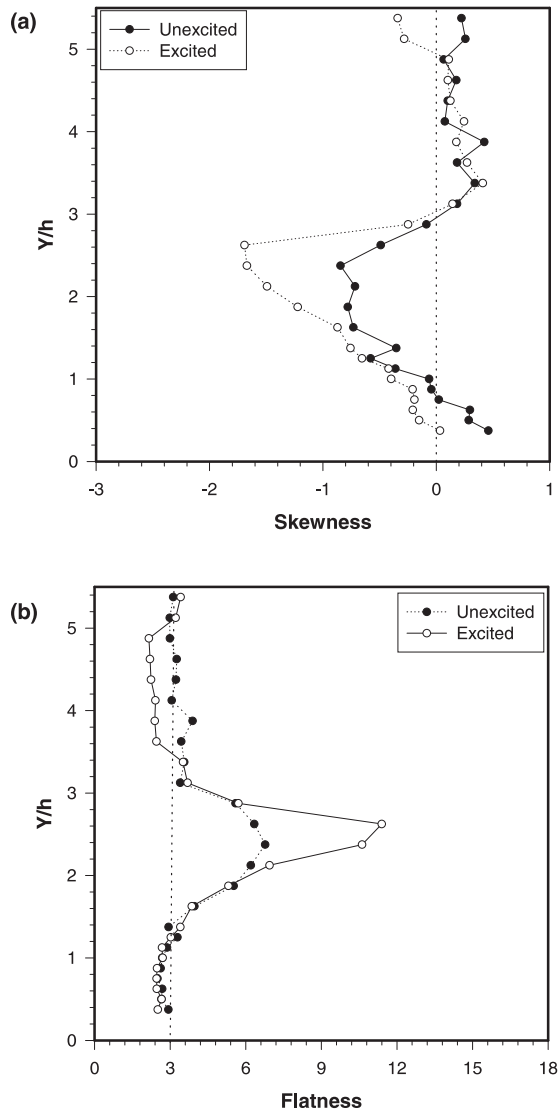


Figure 10. Skewness (a) and flatness (b) profiles of the coherent u -velocity for both unexcited and excited cases at various X/h locations.

similar indicating that the higher order moments and ejection motion are correlated. Thus, the large-scale ejection motion primarily contribute to the non-Gaussian nature of the flow in the outer region of the shear layer.

3.4 Turbulent kinetic energy budget

In the following paragraphs, the turbulent energy budget of the reattaching shear layer behind the surface-mounted rib is presented and comparison is made with the results of the backward-facing step. The turbulent production profiles for the unexcited and excited case at $X/h = 9.0$ are presented in figure 11. Normal stress production can be observed to have its maximum value close to the wall. Normal stress production magnitude is higher than shear stress production magnitude close to the wall resulting in

Table 1. Comparison of Y/h locations for maximum skewness and flatness value with that for maximum average hole size of ejection motion.

X/h	Y/h at maximum skewness and flatness value		Y/h at maximum ejection average hole size value	
	Unexcited case	Excited case	Unexcited case	Excited case
	1.5	1.55	1.6	1.4
4.0	1.6	1.7	1.6	1.6
9.0	2.4	2.6	1.8	2.2

negative total production of turbulent energy which can lead to reduction of turbulence and possibly flow laminarization in this region. For the backward-facing step, Chandrasuda & Bradshaw (1981) also observed the importance of normal stress production compared to shear stress production at close to the wall. From their results, at close to the wall, and at some X/h locations, negative total production can also be inferred. Negative production of turbulent kinetic energy was also observed in an axisymmetric jet (Zaman & Hussain 1980) and a plane mixing layer (Oster & Wygnanski 1982) at certain locations. Hussain (1986) discussed the possibility of negative production for round jet flow in the presence of leap-frog motions of two adjacent vortex rings during the pairing process. If this pairing motion takes place repeatedly at a location, then negative time-average production is observed. These subharmonics are presumably due to the pairing motion of the fundamental wave approaching from upstream. Thus, it may be conjectured that the negative production observed here may be due to leap-frog type of motion of the vortices undergoing pairing. Previously, it was noted that the shear layer developing after reattachment has an inner and outer shear layer with separate origins. Negative production taking place close to the wall is associated with the inner shear layer.

It is also interesting to observe that at the Y/h location of maximum shear stress production ($Y/h \simeq 1.0$) (see figure 11), the normal stress production changes its sign. It may also be pointed out that for a wall jet (Zhou *et al* 1996) similar behaviour between the normal and shear stresses was observed. When excitation is applied, normal production increases while shear production decreases. This may be because large-scale structures get amplified in the near-field region due to excitation and their participation in the pairing process in the reattachment region results in higher values of normal production. Thus, negative production for the excited case is higher than that for the unexcited case. Shear production for the excited case is lower because the velocity gradient is lower in the excited case due to early reattachment. The maximum total production for the unexcited case can be observed to be higher than that of the excited case at $X/h = 9.0$. This explain why the Reynolds stresses were earlier observed to be smaller for the excited cases.

The drop in total production at $X/h = 9.0$ for the excited case should not be taken as an indication that the excitation is responsible for suppressing the turbulence at all locations. Excitation may be responsible for enhancing turbulence in certain regions and suppressing in other regions. To verify this, the turbulent production terms at Y/h locations corresponding to $U/U_{\max} = 0.7$ and 0.9 are plotted for both excited and unexcited cases in figure 12. At $U/U_{\max} = 0.7$, in the early part of the shear layer ($X/h \leq 3.2$), the turbulence production is enhanced by excitation while in the later part of the shear layer the turbulence production is suppressed by excitation. The peak turbulence production is essentially doubled with excitation, and the peak location moves upstream by nearly 2 rib

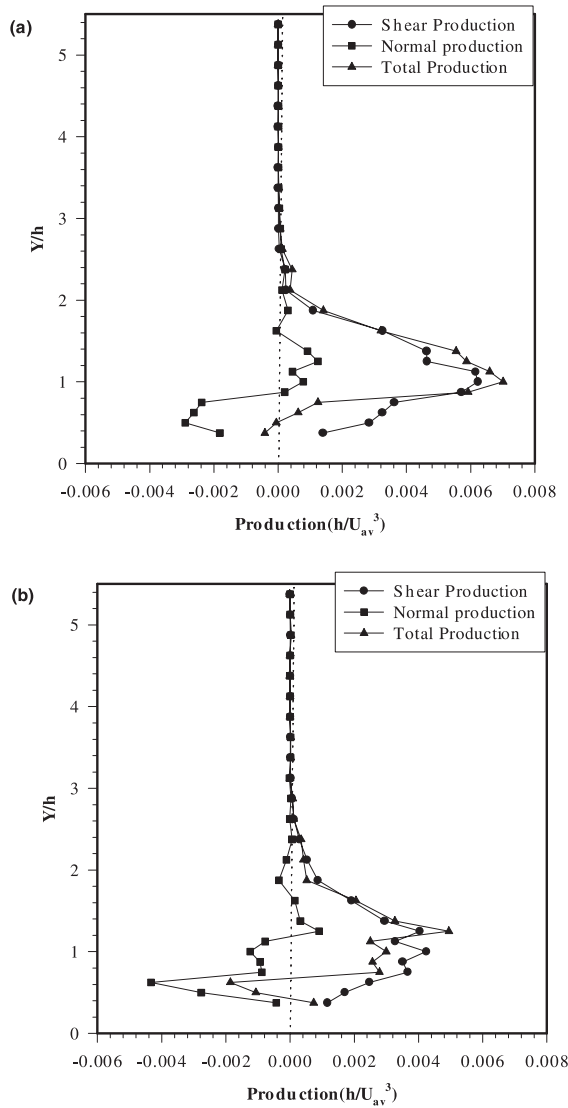


Figure 11. Turbulent energy production at $X/h = 9.0$ for the unexcited case (a) and the excited case (b).

heights representing early reattachment. It is supported by the fact that the reattachment point for the natural case is $5.5h$ and for the excited case is equal to $4.0h$ indicating $1.5h$ reduction in reattachment length for the excited case. Thus the peak turbulence production location and the reattachment location are possibly correlated with each other. Comparing the production at $U/U_{\max} = 0.7$ and $U/U_{\max} = 0.9$, it is observed that at $U/U_{\max} = 0.9$, the effect of excitation on the turbulence production is not as pronounced. The production for the excited case at $U/U_{\max} = 0.9$ is the same order of magnitude as that for the unexcited case. The $U/U_{\max} = 0.7$ and 0.9 locations being away from the wall, the normal stress production does not appear to play a big role in the total production.

Dissipation profiles at $X/h = 9.0$ for both the excited and unexcited cases are presented in figure 13. For both the excited and unexcited cases, the dissipation is observed to

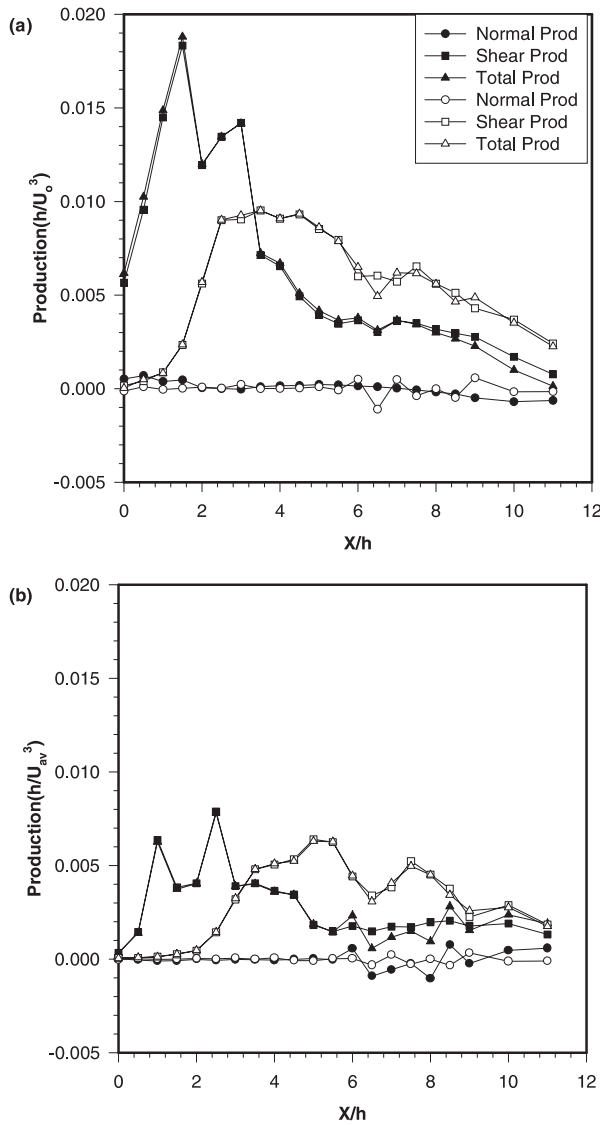


Figure 12. Turbulent energy production at $U/U_{max} = 0.7$ (a) and $U/U_{max} = 0.9$ (b) for both excited and unexcited cases.

be maximum at close to the wall and gradually decreases toward the center of the channel. The dissipation is considerably affected by excitation. The dissipation for the unexcited case is observed to be more than that of the excited case close to the wall. This correlates with the near wall production of turbulence (figure 11), where for $Y/h < 1$, the production values for the excited case are less than those for the unexcited case. Thus, from equilibrium considerations (production = dissipation), a higher dissipation value may be expected near the wall for the unexcited flow case.

Development of the dissipation both before and after reattachment can be observed at Y/h locations corresponding to $U/U_{max} = 0.7$ and 0.9 in figure 14. Dissipation is higher for the excited flow in the near field region. This is consistent with the observation of Favre-Marinet & Binder (1979) who imposed a well-controlled large-scale structure on a round jet and took hot wire measurements on the jet axis. Liu (1981) observed

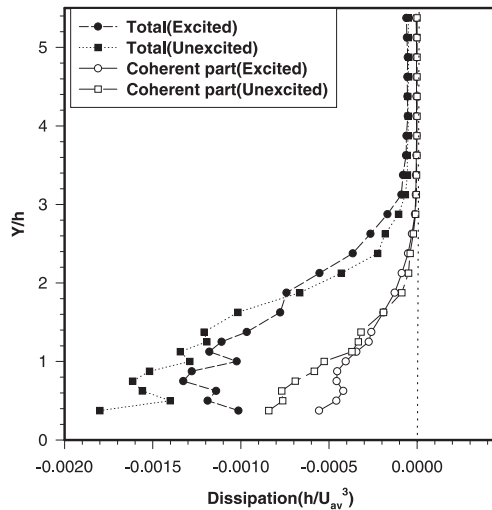


Figure 13. Dissipation profile at $X/h = 9.0$ for both unexcited and excited cases.

that fine-grained turbulence occurs at the expense of the large-scale structures and the turbulent dissipation mechanism is stronger for larger initial level of large-scale structures. Both the large-scale production integral and the viscous dissipation integral of smallest eddies had similar variation. Therefore, it may be argued that, in the present case, the dissipation for the excited case is larger than for the unexcited case, due to higher large-scale magnitude. The dissipation is observed to increase in the downstream direction reaching its maximum value at about the reattachment point. It remains constant around the reattachment region and then decreases with subsequent development of the boundary layer. Maximum dissipation occurs earlier for the excitation case which is consistent with earlier flow reattachment. A distinctive feature of the dissipation profile is the cross-over point at about $X/h = 8$, beyond which the dissipation values for the unexcited cases exceed those for cases with flow excitation.

From the coherent dissipation contribution at $X/h = 9.0$, presented in figure 13, it is observed that the dissipation is not only due to small-scale eddies but also due to the large-scale eddies as opposed to the traditional belief that the dissipation takes place only due to small-scale eddies. Here, the large-scale eddies are found to be equally responsible for dissipation as the small-scale eddies. This observation supports the argument that the participation of large-scale structures amplified by the external excitation results in higher values of dissipation. It is traditionally believed that large eddies are inviscid. However, it is our belief that dissipation takes place due to the interaction among different large-scale eddies and the interaction between large and small-scales. Hussain (1986) observed that even though coherent structure dynamics is essentially inviscid, there is dissipation within the coherent structures, which can be significant. The results obtained and presented here support the prediction of Hussain (1986) regarding the dissipation mechanism.

The combined energy balance for the unexcited and excited cases at $X/h = 9.0$ is shown in figure 15. Pressure transport is observed to play a major role in the turbulent kinetic energy budget for both the excited and unexcited cases. For the unexcited case, the convection and the pressure diffusion are of opposite sign, and further reverse sign at about the same Y/h location (≈ 1.2). Hence, closer to the bottom surface ($Y/h < 1.2$), most of the turbulent energy influx by pressure diffusion and production is either

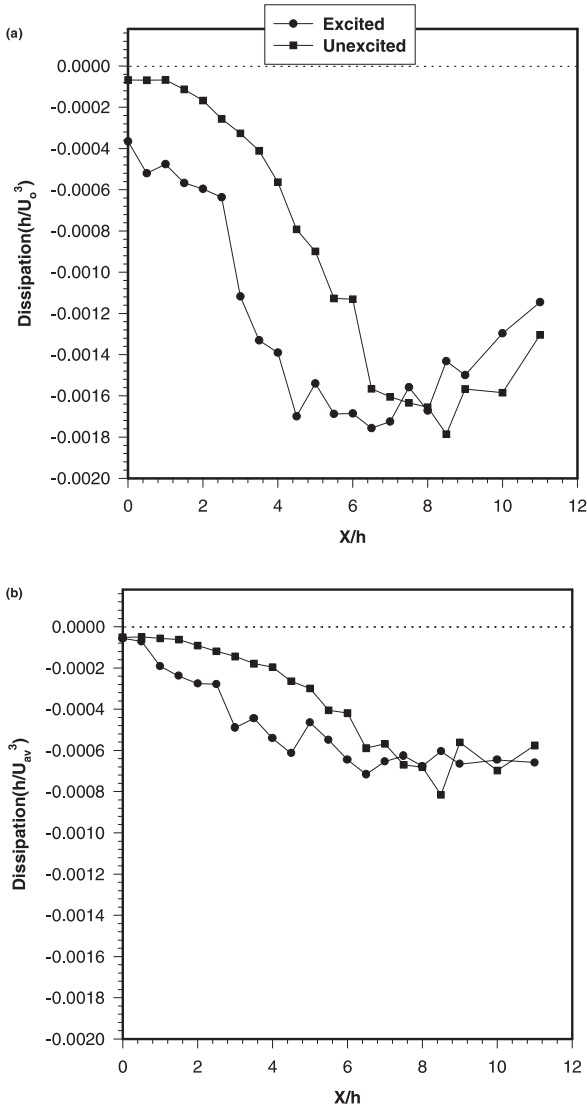


Figure 14. Dissipation profile at $U/U_{max} = 0.7$ (a) and $U/U_{max} = 0.9$ (b) for both unexcited and excited cases.

dissipated or convected away in the downstream direction with the latter mechanism dominating. Away from the wall, the pressure diffusion transport balances the convection, production and diffusion. The pressure diffusion term is observed to be significantly more important than the velocity diffusion. For a wall jet, Zhou *et al* (1996) observed similar variation in pressure transport, i.e. positive gain in turbulent kinetic energy close to the wall and loss away from it. Driver *et al* (1982), assumed the pressure diffusion to be negligible and calculated the dissipation by balance. The significance of the pressure diffusion term observed here indicates that its neglect in order to calculate dissipation by balance (Driver *et al* 1982) may not always be right. For the excited case, at $X/h = 9.0$, the pressure transport and convection contribution do not change their sign at any Y/h location. Both convection and pressure transport are observed to be the most dominant turbulent transport quantities.

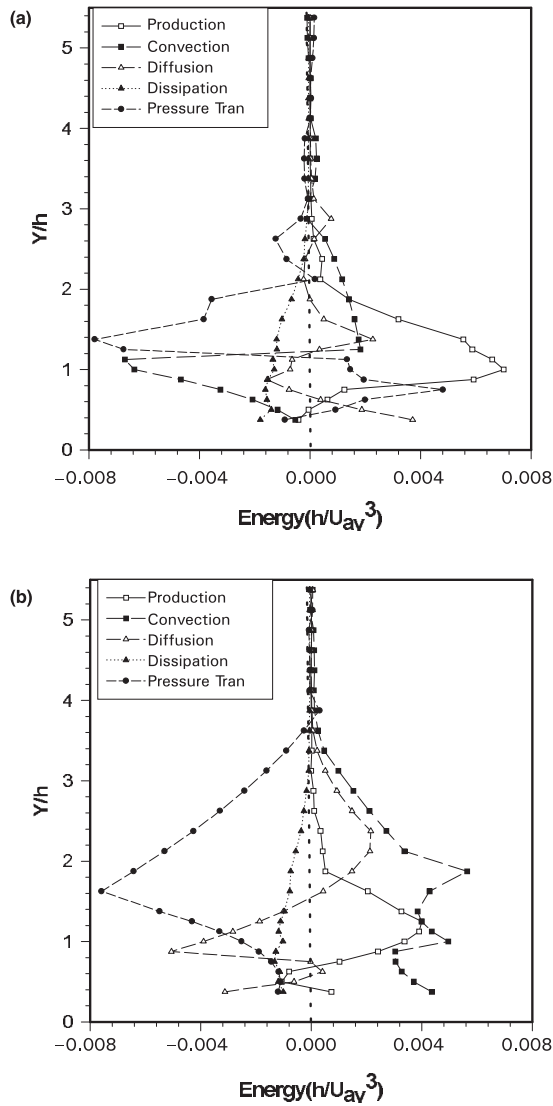


Figure 15. Turbulent kinetic energy budget for the unexcited case (a) and the excited case (b) at $X/h = 9.0$.

3.5 Kinetic energy of coherent eddies

The coherent energy budget terms at $X/h = 9.0$ for both the unexcited and excited cases are presented in figure 16. Comparing the production contribution from the coherent eddies with that of the total production (see figure 15), most of the production is observed to be due to coherent eddies. While comparing the convection contribution for both the cases, the convection contribution is observed to be due to both coherent and non-coherent eddies. Similar observation about coherent convection and production was also observed for wall jet case by Zhou *et al* (1996). For the unexcited case (figure 16), close to the bottom surface, the coherent eddies are observed to contribute towards the random scale motions (as the intermodal production term is negative), which is dissipated subsequently. Away from the wall, the intermodal production term is positive indicating

energy flux from the fine scale to the coherent motion (backscatter). For the excited case (see figure 16), both in the lower and upper part of the shear layer, positive intermodal production is observed. The back scatter observed in the shear layer after reattachment, may be contributing to a renewed organisation of the coherent structures and the presence of large-scale structures well downstream of the reattachment point as observed by Panigrahi & Acharya (1999) from an octant analysis.

The present results further support the observed backscatter behaviour reported by Knight (1981) and by Hussain (1986). Knight (1981) studied the incompressible temporally developing turbulent mixing layer by imposing a weak perturbation consisting of harmonic and subharmonic disturbance on the initial similarity profiles. For a variety of initial perturbation strengths and wavelengths, energy flux from the fine scale to the coherent

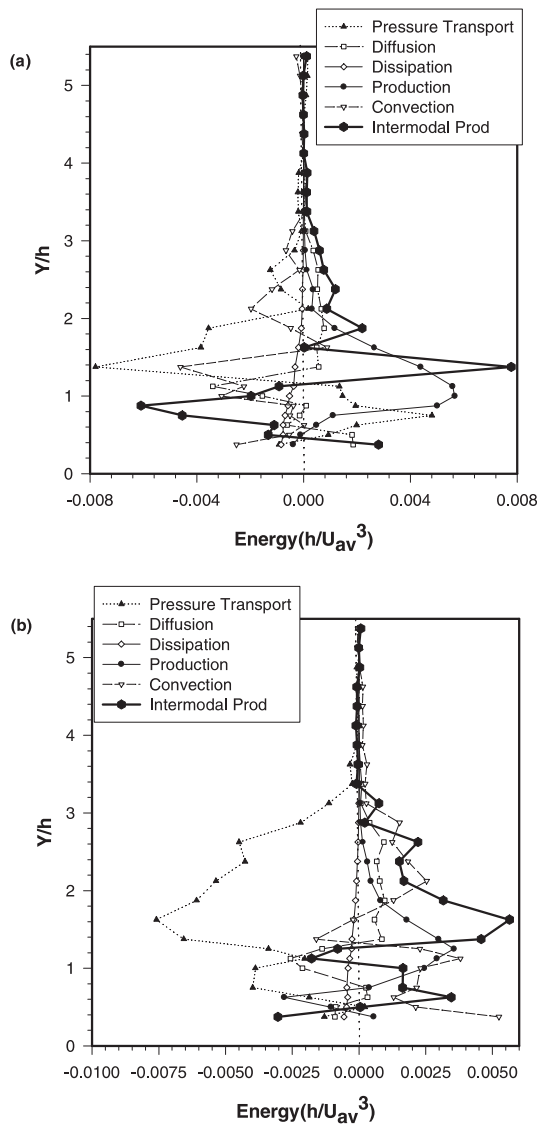


Figure 16. Turbulent kinetic energy budget of the coherent u -velocity for the unexcited case (a) and the excited case (b) at $X/h = 9.0$.

scale was predicted during the pairing process. Hussain (1986), in his review paper about coherent structures, observed that the principal contribution to the coherent vorticity comes from the incoherent field. It was shown that the random stretching of random vorticity fluctuations by random velocity fluctuations ($w_r \cdot \Delta u_r$) and the random advection of random vorticity by random velocity fluctuations ($u_r \cdot \Delta w_r$) can be organised by the coherent structures in such a way as to affect its coherent vorticity.

Note that the intermodal production terms have the largest positive values in the upper part of the shear layers ($Y/h < 1.2$). In this region the velocity is non-Gaussian in nature with higher absolute skewness and flatness values. It was also predicted from quadrant analysis that the large-scale ejection motions were predominant in the upper part of the shear layer. Thus, it seems that in the upper part of the shear layer, the large higher order moments, predominant ejection motions and positive intermodal production are correlated to each other.

4. Conclusion

The near-wall behaviour of reattaching flow behind a rib mounted on the surface of a rectangular channel has been studied experimentally for both excited and unexcited cases. The detailed turbulent structures of the reattaching shear layer developing behind the surface-mounted rib are discussed using the mean velocity profiles, the coherent and random stresses, the higher order moments and the turbulent kinetic energy budget. The following observations are made.

- (1) The coherent structure magnitude obtained from using the pattern recognition method indicates the significance of large-scale coherent structures in the post reattachment region, contrary to the belief that large scales break into small scales, resulting in predominant presence of small scales after the reattachment region.
- (2) The mean velocity profile measurements indicate that X -momentum transport is enhanced in the near wall region due to the excitation at the fundamental frequency. The imposed oscillation mostly affects the coherent part of the total fluctuation.
- (3) The flow past the reattachment point appears to be characterized by an inner layer and an outer layer. These layers appear to have different origins and retain the initial history well past the reattachment point. Thus the re-developing wall flow is distinctly different from that of a flat plate boundary layer flow. This observation is also supported by the Reynolds stress correlation value that is smaller than that of the flat plate boundary layer.
- (4) The higher order moments of the fluctuating u -velocity, i.e. skewness and flatness, are observed to depart from the respective Gaussian value of 0 and 3 in the upper part of the shear layer. This departure is attributed to the large-scale intermittent fluctuation, along the outer edge of the shear layer. The quadrant analysis shows that these large-scale motions in the outer edge of the shear layer are predominantly from ejection motions.
- (5) The dissipation of turbulent kinetic energy has significant contribution from the coherent structures, contrary to the belief that dissipation is a small-scale phenomena. Rather, it is conjectured that dissipation also takes place due to the interaction between different coherent structures.
- (6) The energy budget of the coherent component of turbulent fluctuation shows positive intermodal production in the outer region of the shear layer indicating a reverse cascade mechanism. In the upper shear layer region, the higher order moments, the

large-scale ejection motions and the backscatter phenomena seem to be correlated with one another.

List of symbols

D_h	hydraulic diameter of the channel ($2WH/(W + H) = 0.1013$ m);
f	fundamental frequency;
h	rib height;
H	height of the channel = 0.061 m;
N	total number of samples;
Re	Reynolds number;
u, v, w	streamwise, cross-stream and transverse velocity;
U_{Av}	average velocity in the wind tunnel $\equiv U(W - 2\delta^*)(H - 2\delta^*)/WH$;
U	freestream velocity in the channel;
W	width of the channel = 0.3 m;
X	distance from the downstream edge of the rib in streamwise direction;
Y	distance from channel bottom surface in cross-stream direction;
δ	boundary layer thickness;
μ	dynamic viscosity;
ω	frequency;

Subscripts

c	coherent;
r	random;
f	fundamental component;
s	subharmonic component;
max	maximum;
tot	total.

References

- Bhattacharjee S, Scheelke B, Troutt T R 1986 Modification of vortex interactions in a reattaching separated flow. *AIAA J.* 24: 623–629
- Champagne F H 1978 The fine scale structure of the turbulent velocity field. *J. Fluid Mech.* 86: 67–108
- Chandrasuda C, Bradshaw P 1981 Turbulence structure of a reattaching mixing layer. *J. Fluid Mech.* 110: 171–194
- Driver D M, Seegmiller H L 1982 Features of a reattaching turbulent shear layer subject to an adverse pressure gradient. *AIAA/ASME 3rd Joint Thermophysics, Fluids, Plasma and Heat Transfer Conference*, St Louis, Missouri, AIAA-82-1029
- Favre-Marinet M, Binder G 1979 Structur des jets pulsants. *J. Mech.* 18: 356–394
- Hasan M A Z 1992 The flow over a backward facing step under controlled perturbation: Laminar separation. *J. Fluid Mech.* 238: 73–96
- Hinze J O 1975 *Turbulence* 2nd edn (New York: McGraw-Hill)
- Ho C M, Huere P 1984 Perturbed free shear layers. *Annu. Rev. Fluid Mech.* 16: 365–424
- Hussain A K M F 1970 *The mechanics of a perturbation wave in turbulent shear flow*. Dissertation, Stanford University
- Hussain A K M F 1986 Coherent structures and turbulence. *J. Fluid Mech.* 173: 303–356

- Hussain A K M F, Zaman K B M Q 1980 Vortex pairing in a circular jet under controlled excitation. *J. Fluid Mech.* 101: 493–544
- Knight D D 1981 Numerical investigation of large-scale structures in the turbulent mixing layer. *Symposium on Turbulence Proceedings of the Sixth Symposium on Turbulence in Liquids*, Department of Chemical Engineering, University of Missouri-Rolla, pp 167–177
- Kundu P K 1990 *Fluid mechanics* (New York: Academic Press)
- Liu J T C 1981 Interaction between large-scale coherent structures and fine-grained turbulence in free shear flows. *Transition Turbulence*: 167–214
- Lumley J L 1981 Coherent structures in turbulence. *Transition Turbulence*: 215–242
- Oster D, Wygnanski I 1982 The forced mixing layer between parallel streams. *J. Fluid Mech.* 123: 91–130
- Panigrahi P K 2001 Fundamentally excited flow past a surface-mounted rib. Part I: Turbulent structures characterization. *Sadhana* (this issue)
- Panigrahi P K, Acharya S 1999 Mechanisms of turbulence transport in a turbine blade coolant passage with a rib turbulator. *J. Turbomachinery* 121: 152
- Roos F W, Kagelman J T 1986 Control of coherent structures in reattaching laminar and turbulent shear layers. *AIAA J.* 24: 1956–1963
- Zaman K B M Q, Hussain K M F 1980 Vortex pairing in a circular jet under controlled excitation Part I. General jet response. *J. Fluid Mech.* 101: 449–491
- Zhou M D, Heine C, Wygnanski I 1996 The effects of excitation on the coherent and random motion in a plane wall jet. *J. Fluid Mech.* 310: 1–37